Double photoionization of two-electron atoms based on the explicit separation of dominant ionization mechanisms

Tobias Schneider and Jan-Michael Rost*
Max Planck Institute for the Physics of Complex Systems, Nöthnitzer Straße 38, 01187 Dresden, Germany
(Received 21 February 2003; published 11 June 2003)

Double ionization by a single photon is often discussed in terms of two mechanisms, namely, *shakeoff* and *knockout*, dominant at high and low photon energies, respectively. We have developed a model to formulate the explicit but separate contribution of both mechanisms at all energies [Phys. Rev. Lett. **89**, 073002 (2002)]. The separation is based on a quasiclassical formulation of knockout which is free from any shakeoff part since the latter is purely quantum mechanical. The relevance of each mechanism from threshold up to several keV photon energy is quantified and discussed in detail for the photoionization from the ground state of two-electron atoms. Photoionization ratios, integral and singly differential cross sections calculated for helium and other members of its isoelectronic sequence are compared to benchmark experimental data and recent theoretical results. A connection to Samson's half-collision model [Phys. Rev. Lett. **65**, 2861 (1990)] is also given.

DOI: 10.1103/PhysRevA.67.062704 PACS number(s): 32.80.Fb, 03.65.Sq, 34.80.Dp

I. INTRODUCTION

The escape of two electrons from an atom or ion due to the absorption of a single photon cannot be understood in the framework of independent particles. Since the electron-photon coupling is of single-particle nature, only the electron-electron correlation renders such a process possible. This explains the interest in double photoionization of the simplest many-electron atom, namely, helium, or more generally the two-electron atom documented through an extensive literature on the subject, including theoretical [1–12] as well as experimental work [13–18]. On the theoretical side, only in recent years, sophisticated *ab initio* methods have been developed which allow for an exact treatment of the two outgoing correlated electrons [19–21]. Exactly these final-state correlations are the most challenging issue in theoretical *ab initio* investigations. Some of these calculations are in excellent agreement with experiment for both, integral and differential, cross sections. Nevertheless, the underlying ionization mechanism remains difficult to uncover within such fully numerical approaches. Hence, suitable approximate calculations [22,23] that reveal the dynamical mechanisms can supplement the accurate numerical results to complete the theoretical picture of double photoionization.

After the initial absorption of the photon by the primary electron, the subsequent redistribution of the energy among the two electrons is often discussed in terms of two separate mechanisms [18,22–26], knockout (KO) and shakeoff (SO). The first mechanism (sometimes called ''two-step-one'' [27]) describes the correlated dynamics of the two electrons as they leave the atom where the primary electron (the photoelectron) is knocking out the secondary electron in an $(e,2e)$-like process. It is the final-state correlation that governs the knockout mechanism. On the other hand, the shakeoff mechanism [6–9,28] accounts for the fact that absorption of the photon may lead to a sudden removal of the photoelectron without any direct interaction with the secondary electron. This causes a change in the atomic field so that the secondary electron relaxes with a certain nonvanishing probability to an unbound state of the remaining He^+ ion, i.e., the secondary electron is shaken off. Here, the initial-state correlations are important, i.e., the correlations present in the system before the photon has been absorbed.

The clearest and most symmetric distinction of these mechanisms is provided in a perturbative approach where not only the coupling to the photon is treated perturbatively (as usual) but also the electron-electron interaction. If double photoionization is represented by Feynman diagrams [23,25,29] KO differs from SO by the chronological order of photoabsorption and electron-electron interaction. While for SO the electron correlation takes place before the photoabsorption, it is the exact opposite for KO. Unfortunately, this clear formulation and distinction of the processes cannot be used for an accurate calculation since taking into account the electron-electron interaction only perturbatively is not a satisfactory approximation.

Based on the qualitative picture described above one may also distinguish KO and SO by the different interaction times or the different energy regimes where they dominate. SO is characterized by a sudden removal of the photoelectron and therefore by a short, even vanishing time of interaction between the ionized electrons. This situation is typical for the high-energy regime with photons of short wavelength. On the other hand, KO dominates for low photon energies near threshold when the electrons have little energy in the continuum and therefore plenty of time for interaction.

However, apart from the prevalence of shakeoff at high photon energies these criteria do not provide means to separate the mechanisms. Moreover, being only defined rigorously in the limit of infinite photon energy it is not obvious, and certainly no unique solution exists, how to extrapolate shakeoff to finite photon energies [24,30,31].

Yet, there exists another classification that can help to separate KO and SO and this is their respective quantum character. SO is a pure quantum phenomenon, namely, an

*Electronic address: rost@mpipks-dresden.mpg.de

overlap of two wave functions which belong to different Hamiltonians (sudden approximation), and no classical equivalent exists. Hence, if one is able to formulate KO semiclassically based on classical input only, it will not contain any SO contribution. Viewed from a different, more semiclassical perspective: A semiclassical formulation of photoionization lacks the purely quantum-mechanical SO contribution that needs to be added as a correction for a meaningful description.

In the following, we will describe in detail how we have realized the theoretical concept described above for the double photoionization of two-electron atoms or ions from the (symmetric) ground state. Our guiding principle has been a formulation with the least possible numerical effort having in mind to extend our approach to three-electron atoms in the future. For knockout, this implies a quasiclassical description. This is an additional simplification compared to a full semiclassical calculation since the two electrons are propagated classically with their full interaction but the initial phase-space distribution is formulated in terms of the quantum wave function.

We formulate SO and KO in terms of the probability to find two simultaneously free electrons after absorption of the photon. In this context, it is convenient to express the double-ionization cross section as

$$\sigma_X^{++} = \sigma_{\rm abs} P_X^{++}, \tag{1}$$

where X stands for either shakeoff or knockout and $\sigma_{\rm abs}$ denotes the total photoabsorption cross section. We will calculate the double escape probabilities P_X^{++} from the ground state. For $\sigma_{\rm abs}$, we can either use the experimental data of Samson *et al.* [32] or the analytical result from Ref. [33].

The paper is organized as follows. In Sec. II, we present our classical-trajectory Monte Carlo (CTMC) phase-space method for knockout. CTMC is a tool which has been frequently used for particle impact induced fragmentation [34–37] and also for ionization in strong fields [38–40] with implementations typically differing in the way the phase-space distribution $\rho(\Gamma)$ is constructed. In Sec. III, we interpret our KO results in terms of Samson's half-collision model. Our approach to shakeoff is described in Sec. IV. It is based on Åberg's formula [6]. In Sec. V, we present our results for integral cross sections for helium and its isoelectronic sequence, and in Sec. VI, we discuss the results for the singly differential cross sections in comparison with recent experimental data. We will also address the lack of interference terms. Finally, the paper ends with a summary in Sec. VII.

II. KNOCKOUT IONIZATION

After the photon has transferred all its energy to the primary electron the subsequent evolution of the two electrons resembles an electron-impact induced collision, a fact that will be discussed in detail in Sec. III. We formulate this evolution quasiclassically by expressing the double-ionization probability of Eq. (1) as [41]

$$P_{\rm KO}^{++} = \lim_{t\to\infty} \int d\Gamma_{\mathcal{P}^{++}} \exp[(t-t_{\rm abs})\mathcal{L}_{\rm cl}]\rho(\Gamma), \tag{2}$$

where $\mathcal{L}_{\rm cl}$ denotes the classical Liouvillian corresponding to the classical three-body Coulomb Hamiltonian H and $t_{\rm abs}$ is the time of absorption that triggers the classical propagation. The projector $\mathcal{P}^{++}$ indicates that the integration has to be performed only over those parts of the phase space $\Gamma_{\mathcal{P}^{++}}$ that lead to double escape, i.e., where the asymptotic energies of the two electrons are positive. The integral in Eq. (2) is evaluated with a standard Monte Carlo technique that entails following classical trajectories in phase space. The photon energy ω determines the excess energy E in phase space for which the dynamics of the two electrons takes place

$$E = \omega - I^{++}, \tag{3}$$

where I^{++} is the two-electron binding energy.

As mentioned before charged particle impact processes have been described successfully with CTMC phase-space methods. While all the methods share the classical propagation in time they typically differ in the way the initial state is modeled, e.g., purely classically as a phase-space distribution on a torus or quantum mechanically, e.g., by a Wigner distribution. Our initial distribution $\rho(\Gamma)$ is the two-electron density immediately after photon absorption at time $t_{\rm abs}$,

$$\rho(\Gamma) = N\,\delta(\boldsymbol{r}_1)\rho_2(\boldsymbol{r}_2,\boldsymbol{p}_2), \tag{4}$$

where N is a normalization constant. With $\delta(\boldsymbol{r}_1)$, we assume the absorption to happen directly at the nucleus [24]. This PEAK (primary electron at the nucleus) approximation becomes exact in the limit of high photon energy [42].

Regularized coordinates [43] are used to avoid problems which arise from starting at the nucleus ($\boldsymbol{r}_1 = 0$). The PEAK approximation significantly reduces the initial phase-space volume to be sampled. Furthermore, it allows one to match the energy condition Eq. (3) for the starting configurations such that the two electrons can be treated separately since the photoelectron at the nucleus can have any energy necessary to add up to the excess energy E together with the energy of the secondary electron contained in its phase-space distribution

$$\rho_2(\boldsymbol{r}_2,\boldsymbol{p}_2) = \mathcal{W}_\psi(\boldsymbol{r}_2,\boldsymbol{p}_2)\,\delta(\varepsilon_2^{\rm in} - \varepsilon_B). \tag{5}$$

In Eq. (5), $\mathcal{W}_\psi(\boldsymbol{r}_2,\boldsymbol{p}_2)$ is the Wigner distribution function of the two-electron wave function with electron 1 at the nucleus,

$$\psi(\boldsymbol{r}_2) = \frac{\Psi_0(\boldsymbol{r}_1=0,\boldsymbol{r}_2)}{[\langle\Psi_0(\boldsymbol{r}_1=0,\boldsymbol{r}_2)|\Psi_0(\boldsymbol{r}_1=0,\boldsymbol{r}_2)\rangle]^{1/2}}. \tag{6}$$

Since we consider absorption from the ground state, $\Psi_0(\boldsymbol{r}_1,\boldsymbol{r}_2)$ is the helium ground-state wave function. Here and in the following, the brackets indicate integration with respect to the secondary electron. We call Eq. (5) a *restricted* Wigner distribution since the initial energy of the secondary electron, $\varepsilon_2^{\rm in}$ has been fixed to the shell ε_B. Taking advantage

of the fact that for the KO mechanism the initial-state correlations are not so important, we represent the helium ground state by the independent particle wave function $\Psi_0(\boldsymbol{r}_1,\boldsymbol{r}_2) = (Z_{\rm eff}^3/\pi)\exp[-Z_{\rm eff}(\boldsymbol{r}_1+\boldsymbol{r}_2)]$ with effective charge $Z_{\rm eff}=Z-5/16$ [23]. From this follows simply $\varepsilon_2^{\rm in}=\boldsymbol{p}_2^2/2-Z_{\rm eff}/r_2$ and for future reference, we also note that the binding energy of the secondary electron is given by $\varepsilon_B=-Z_{\rm eff}^2/2$.

The formulation of the knockout probability may seem to involve a lot of approximations whose effect is not easy to control. In this situation, the relation of the KO probability to electron-impact ionization offers a testing ground suitable to assess the performance of Eq. (2) with the input of Eqs. (4)–(6).

III. RELATION TO SAMSON'S HALF-COLLISION MODEL

Samson [10] and later in a more elaborate way by including shakeoff Pattard and Burgdörfer [24] have related double photoionization of a two-electron atom A,

$$A+\gamma\rightarrow A^{++}+2e^-, \tag{7}$$

to electron-impact ionization of the corresponding positively charged ion,

$$A^+ + e^- \rightarrow A^{++}+2e^-. \tag{8}$$

Looking at the right-hand side of Eqs. (7) and (8) the two processes lead, in the chemists' language, to the same ''products.'' In particular, as Samson pointed out, the emission of the secondary electron in the photoionization process should resemble the electron-impact ionization by the primary (photo) electron. As a consequence, it has been proposed [10,24,26] that the electron-impact ionization cross section σ_e should be proportional to the double-photoionization probability P^{++},

$$P^{++}(E)=C\sigma_e(E), \tag{9}$$

where the constant C has the unit of an inverse cross section. The excess energy E is measured from the (single-) ionization threshold of A^+ on the right-hand side (rhs) and from the double-ionization threshold of the two-electron atom A on the left-hand side. The connection of the two processes, condensed in Eq. (9), is sometimes referred to as the half-collision picture of double photoionization. The term ''half collision'' draws its justification from the observation that in photoionization the first half of the collision, i.e., the incoming motion of the impacting electron, is missing (see Fig. 1). Obviously, the half-collision model is identical to the knockout picture from the preceding section. On the other hand, this implies a rather limited validity of Eq. (9), if the *full* photoionization probability (KO and SO) is used. Clearly, SO is not present in electron-impact ionization of the corresponding ion [24,26]. On the other hand, SO even dominates double photoionization for high excess energies. Hence, the half-collision model in the form of Eq. (9) must fail for increasing excess energy. Pattard and Burgdörfer [24] remedied this failure by explicitly introducing a shakeoff term on the rhs of Eq. (9).

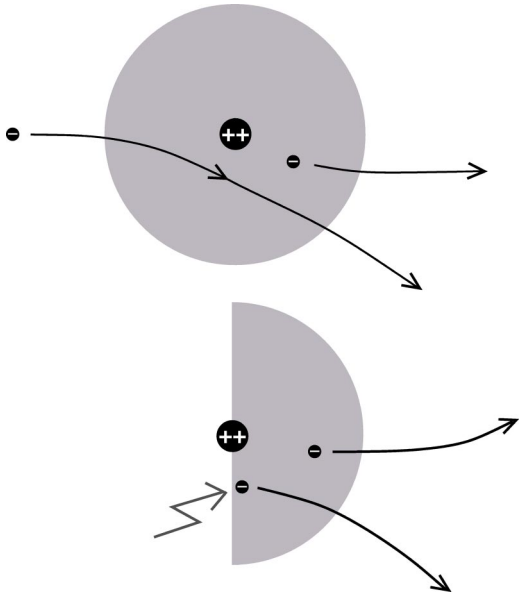

FIG. 1. Schematic representation of the half-collision picture. The upper part shows electron-impact ionization (full collision). The lower part depicts the knockout mechanism (half collision). The flash symbolizes the photon that is absorbed by one of the electrons.

We do not need this correction term since the knockout probability Eq. (2) is not ''polluted'' by any shakeoff contribution. According to the half-collision concept, we would expect that a modified Eq. (9), where P^{++} is replaced by $P_{\rm KO}^{++}$, should hold for the whole energy range, from threshold to some 1000 eV. Figure 2(a) shows $P_{\rm KO}^{++}$ for helium compared to the experimental cross section of the electron-

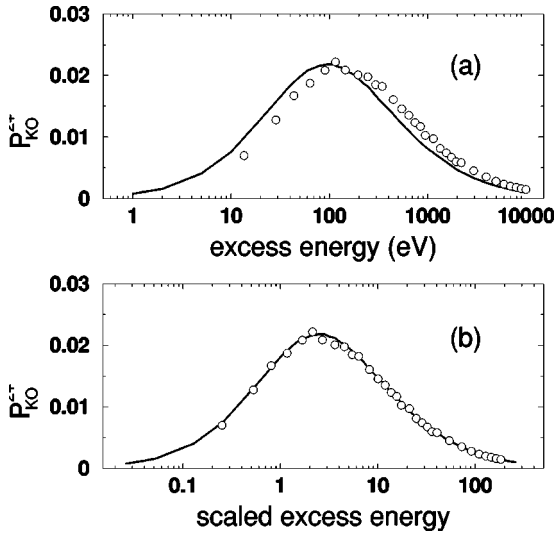

FIG. 2. $P_{\rm KO}^{++}$ for the helium atom (solid line) compared to the cross section for electron-impact ionization of He^+ [44] (circles) (a) according to Eq. (9) and (b) according to Eq. (10). The constant C in Eqs. (9) and (10) is given by $C=4.67\times10^{15}$ cm^{-2}.

impact ionization of He^+ by Peart *et al.* [44]. The two curves have a similar shape but they seem to be shifted with respect to each other in energy indicating that the replacement of P^{++} by P^{++}_{KO} in Eq. (9) is not the only modification that is necessary to link our knockout results to electron-impact ionization. So far we have not taken into account the different energy scales which are inherent in the two processes and which are set by the respective bound electron. On the one hand, for impact ionization the target electron in the He^+ ion is bound by $E_B=-Z^2/2$, while the photoionization KO process from Sec. II involves an electron with half the ground-state energy $E'_B=-Z^2_{\rm eff}/2=-(Z-5/16)^2$, i.e., the nuclear charge is screened for each electron in the ground state of a two-electron atom. These considerations lead us to the following modified version of Eq. (9):

$$P^{++}_{\rm KO}(2E/Z^2_{\rm eff})=C\sigma_e(2E/Z^2), \tag{10}$$

where E again denotes the appropriate excess energy. Figure 2(b) shows the rescaled KO probability $P^{++}_{\rm KO}(2E/Z^2_{\rm eff})$ for the helium atom compared to the rescaled experimental impact ionization data $\sigma_e(2E/Z^2)$ for the He^+ ion. As one can clearly see Eq. (10) is valid over the whole energy range for which the experimental impact ionization data is available (up to $E=10$ keV excess energy). In the case of helium, the constant C is given by $C=4.67\times10^{15}$ cm^{-2}.

For the other members of the helium isoelectronic sequence Eq. (10) holds as well (not shown here). For increasing nuclear charge Z, the two different energy scales, E_B and E'_B, come closer with $E_B/E'_B\to1$ as $Z\to\infty$ since in this limit there is no screening of the nuclear charge through other electrons.

We may summarize that the half-collision model offers support for the formulation of the knockout probability of Eq. (2) and vice versa, the KO probability for double photoionization is in excellent agreement with the impact ionization of the corresponding ion, justifying the idea of the half-collision model.

IV. SHAKEOFF IONIZATION

In contrast to the knockout mechanism, shakeoff cannot be understood in a classical framework. However, it does not elude a simple quantum-mechanical treatment as KO does. The initial-state correlations that characterize the SO mechanism are much easier to handle than the final-state correlations in the case of KO. What remains difficult, however, is the extrapolation of shakeoff to finite photon energies. Several other schemes have been proposed in the literature, e.g., Refs. [24,30,31].

As a generalization of the well-known formula for the shake mechanism valid at very high energies [6,7], Åberg gave an expression for the probability to find the shake electron (i.e., the secondary electron) in a hydrogenic eigenstate of the bare nucleus ϕ_α at *any* excess energy [6],

$$P^{\nu}_{\alpha}=\frac{|\langle\phi_\alpha|\psi^\nu\rangle|^2}{\langle\psi^\nu|\psi^\nu\rangle}, \tag{11}$$

with

$$\psi^\nu(\boldsymbol{r}_2)=\int d^3r_1\,\nu^*(\boldsymbol{r}_1)\Psi_0(\boldsymbol{r}_1,\boldsymbol{r}_2), \tag{12}$$

where $\nu(\boldsymbol{r}_1)$ is the wave function of the primary (photo)electron after it has left the atom. If it was in an s state before the absorption, it is in a p state afterwards. The secondary (shake) electron does not change its angular momentum. In Eq. (12), $\Psi_0(\boldsymbol{r}_1,\boldsymbol{r}_2)$ again denotes the two-electron ground-state wave function. Note that ϕ_α might either be a bound state ($\alpha=n$) or a continuum state ($\alpha=\varepsilon$). (Note also that in the case of an energy-normalized continuum state, P^ν_ε has the unit of probability per energy.)

In the high-energy limit, the ejected primary electron may be described by a plane wave,

$$\nu(\boldsymbol{r}_1)=(2\pi)^{-3/2}\exp(-i\boldsymbol{k}_1\cdot\boldsymbol{r}_1). \tag{13}$$

In that case, $\psi^\nu(\boldsymbol{r}_2)$ is just the Fourier transform of the ground-state wave function with respect to $\boldsymbol{r}_1$ [cf. Eq. (12)]. Due to the large momentum $k_1\gg0$ of the primary electron, Eq. (12) and subsequently Eq. (11) can be further simplified. One easily finds

$$P_\alpha=\frac{|\langle\phi_\alpha|\Psi_0(\boldsymbol{r}_1=0,\boldsymbol{r}_2)\rangle|^2}{\langle\Psi_0(\boldsymbol{r}_1=0,\boldsymbol{r}_2)|\Psi_0(\boldsymbol{r}_1=0,\boldsymbol{r}_2)\rangle}, \tag{14}$$

where we have used the following two properties [6]:

$$k_1^4\psi^\nu(\boldsymbol{r}_2)\approx-2(2/\pi)^{1/2}\frac{\partial\Psi_0}{\partial r_1}\Big|_{r_1=0} \tag{15}$$

(valid for large k_1) and

$$\left.\frac{\partial\Psi_0}{\partial r_1}\right|_{r_1=0}=-2\Psi_0(\boldsymbol{r}_1=0,\boldsymbol{r}_2). \tag{16}$$

The latter property is known as one of Kato's cusp conditions [45]. Equation (14) is the well-known asymptotic shake probability [6,7]. Formally, the wave function ψ^ν has been replaced by $\Psi_0(\boldsymbol{r}_1=0,\boldsymbol{r}_2)$ in Eq. (14). If we assume this replacement to be valid for all excess energies, i.e., if we perform the PEAK approximation as in the case of KO, the double-photoionization probability from shakeoff at any finite excess energy E is given by

$$P^{++}_{\rm SO}(E)=\int_0^\infty d\varepsilon'\int_0^\infty d\varepsilon P_\varepsilon\,\delta(E-\varepsilon'-\varepsilon), \tag{17}$$

where ε' denotes the kinetic energy of the primary electron after having left the atom and ε the energy of the shaken electron, as before ($\varepsilon',\varepsilon>0$). Note that the δ function in Eq. (17) ensures the conservation of the total energy. Using Eq. (14), we are left with

$$P^{++}_{\rm SO}(E)=\int_0^E d\varepsilon P_\varepsilon, \tag{18}$$

TABLE I. Effective shake charges Z_S and effective shake screening $\delta_S = Z - Z_S$ for some members of the helium isoelectronic sequence (see text). The asymptotic double-to-single ratios are taken from Forrey *et al.* [8].

Z	R_∞	Z_S	δ_S
2	0.01645	1.494	0.506
3	0.00856	2.483	0.517
4	0.00508	3.480	0.520
5	0.00334	4.479	0.521
6	0.00236	5.478	0.522
7	0.00175	6.477	0.523
8	0.00135	7.477	0.523
9	0.00107	8.477	0.523
10	0.00087	9.477	0.523

which for high energies gives the standard asymptotic shakeoff probability [7–9]

$$P_{\mathrm{SO}}^{++}(E\to\infty) = \int_0^\infty d\varepsilon P_\varepsilon = 1 - \sum_n P_n . \tag{19}$$

To simplify the calculation of shakeoff further, we replace $\Psi_0(\boldsymbol{r}_1 = 0, \boldsymbol{r}_2)$ in Eq. (14) by a normalized hydrogenic wave function $\psi_{1s}^{Z_S}(\boldsymbol{r}_2)$ where the initial-state correlations of the two electrons are absorbed into an effective shake charge Z_S,

$$\tilde{P}_\alpha = |\langle \phi_\alpha | \phi_{1s}^{Z_S} \rangle|^2 . \tag{20}$$

To our knowledge, an effective charge in connection with SO was first introduced by Surić, Pisk, and Pratt [46] only recently. We choose the effective charge Z_S in such a way that

$$\int_0^\infty d\varepsilon \tilde{P}_\varepsilon = \frac{R_\infty}{1+R_\infty}, \tag{21}$$

where R_∞ is the exact asymptotic double-to-single ratio $R_\infty = [P^{++}/(1-P^{++})]_{E\to\infty}$ which is determined by SO only. For the members of the helium isoelectronic sequence, R_∞ can be found in the literature [8,9]. We find Z_S to be $2 - 0.51$ in the case of the helium atom ($R_\infty = 0.016\,45$ for the ionization from the helium ground state). For helium, we have found little difference for the shakeoff probability as a function of excess energy between this simple ansatz, i.e., using Eq. (20), and a fully correlated Hylleraas wave function [47] for Ψ_0, i.e., using Eq. (14). The difference mainly originates from the slightly different asymptotic ratio that is obtained with the Hylleraas function we took for Ψ_0 in contrast to the $R_\infty = 0.016\,45$ used in Eq. (21).

In Table I, we have listed the effective shake charge Z_S for helium and some other members of its isoelectronic sequence. With increasing Z (where Z is the charge of the bare nucleus) the shake charge appears to converge towards $Z_S \approx Z - 0.52$. We note that Z_S is quite different from the ''standard'' $Z_{\mathrm{eff}} = Z - 5/16$ we used in our calculation of the KO process before. As it is well known, using Z_{eff} instead of Z_S on the right-hand side of Eq. (21) leads to a value for the asymptotic ratio that is too much low. In the case of helium, for instance, one finds a value of 0.0072 (compared to the correct value of $R_\infty = 0.016\,45$). This discrepancy is to be expected since Z_{eff} represents the screened nuclear charge that both ground-state electrons see ''on average'' in a completely symmetric fashion. For the shakeoff process, this symmetry is broken since one electron (called the primary electron) absorbs the photon whereas the second one acts as a spectator only. One might even think that an extreme value of $Z-1$ for the effective shake charge would be more adequate for a description of SO since the primary electron located at the nucleus when absorbing the photon should screen the nucleus for the secondary electron in the most efficient way. However, it turns out that using $Z-1$ in Eq. (21) overestimates the asymptotic ratio noticeably. The effective charge Z_S lies between $Z-1$ and $Z_{\mathrm{eff}} = Z - 5/16$.

We would like to emphasize that the use of effective shake charges would not be necessary in the present context of two-electron systems. We could (have) calculated the shake probability with the full ground-state wave function. However, for three-electron systems the effort increases already considerably and in connection with the PEAK approximation (i.e., evaluation of the initial-state wave function at the nucleus for the photoelectron) the use of effective shake charges for the remaining orbital is a natural approximation.

V. INTEGRAL CROSS SECTIONS

Combining the KO and SO contributions, calculated as described in the last sections, we are led to the double-photoionization probability [22]

$$P^{++} = P_{\mathrm{KO}}^{++} + P_{\mathrm{SO}}^{++} . \tag{22}$$

From a classical (nonquantum-mechanical) point of view the knockout process is the only mechanism that leads to double ionization after the absorption of a single photon. In Eq. (22), P_{SO}^{++} may therefore be viewed as a quantum correction to the quasiclassically calculated double photoionization given by KO. In our description of KO, quantum features enter only indirectly through the use of the phase-space distribution function $\rho(\Gamma)$ which describes the initial (nonclassical) state of the atom before the classical ionization process takes place. According to Eq. (1), the integral double-ionization cross section is given by

$$\sigma^{++} = \sigma_{\mathrm{abs}}(P_{\mathrm{KO}}^{++} + P_{\mathrm{SO}}^{++}) \equiv \sigma_{\mathrm{KO}}^{++} + \sigma_{\mathrm{SO}}^{++} . \tag{23}$$

The single-ionization cross section can be written as $\sigma^+ = \sigma_{\mathrm{abs}} - \sigma^{++}$, whereas the double-to-single ratio can be expressed without referring to σ_{abs},

$$R = \sigma^{++}/\sigma^+ = P^{++}/(1-P^{++}), \tag{24}$$

with P^{++} given in Eq. (22).

A. Helium

In Fig. 3, we compare the cross section for the double photoionization of the ground-state helium atom to the ex-

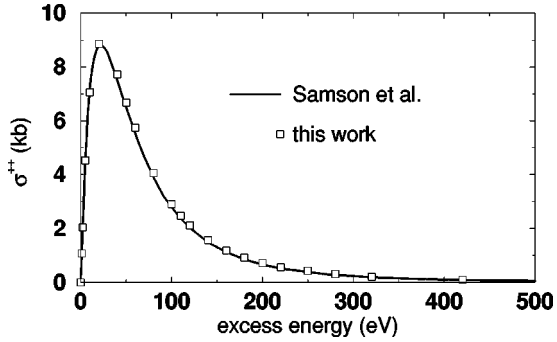

FIG. 3. Double-photoionization cross section. Open rectangles: our theoretical results. Full line: experimental data of Samson *et al.* [15].

perimental data of Samson *et al.* [15]. For the whole energy range shown in Fig. 3, we find an excellent agreement. As already mentioned in the Introduction, the experimental data of Samson *et al.* [32] is used for $\sigma_{\rm abs}$ which is believed to be very precise. Instead we could have used the analytic expression for $\sigma_{\rm abs}$ from Ref. [33], leading to a similar result for σ^{++}.

Figure 4 shows the double-to-single ratio for helium compared to the benchmark experimental data of Samson *et al.* [15], and additionally, to other theoretical data [5,4,20], calculated by means of large-scale computer codes. Again, we note very good agreement. In the inset of Fig. 4, we show the double-to-single ratio for a larger energy range. In addition to the complete ratio, Eq. (4), we also present the ratios calculated by considering only one of the two mechanisms, KO or SO,

$$R_X = P_X^{++}/(1-P_X^{++}), \tag{25}$$

where X again stands for either knockout or shakeoff [22].

B. Helium isoelectronic sequence

We can apply our model not only to the helium atom but also to the members of its isoelectronic sequence. Only the charge of the nucleus Z has to be changed appropriately.

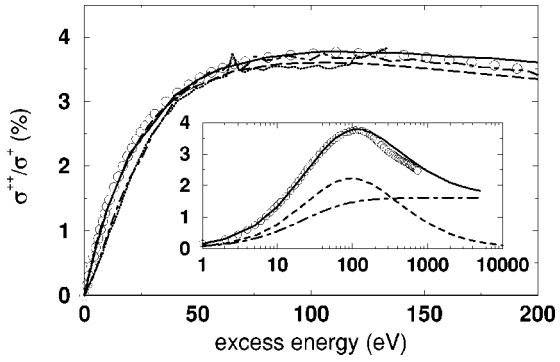

FIG. 4. Helium photoionization double-to-single ratio. Circles: experimental data of Samson *et al.* [15]. Full line: our result. Dashed line: CCC data of Kheifets and Bray [20]. Dotted line: *R*-matrix data of van der Hart and Feng [4]. Dot-dashed line: *R*-matrix data of Meyer *et al.* [5]. Inset, circles and full line as before; dashed line, our approach, knockout mechanism only; dot-dashed line, shakeoff mechanism only (see text).

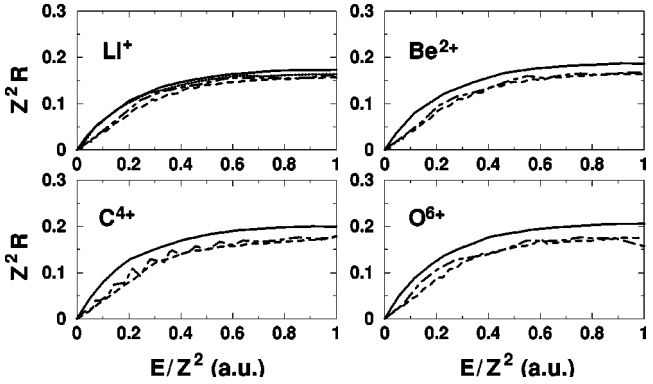

FIG. 5. Photoionization double-to-single ratio for (a) Li^+, (b) Be^{++}, (c) C^{4+}, and (d) O^{6+}. Full line: present results. Dashed line: van der Hart and Feng [4]. Dot-dashed line: Meyer *et al.* [5]. Dotted line (Li^+ only): Kheifets and Bray [20].

As was pointed out by Kornberg and Miraglia [48] the double-photoionization cross sections σ_Z^{++} of the isoelectronic sequence should (approximately) obey the following scaling relation:

$$\sigma_Z^{++}(E) = f_1(E/Z^2)/Z^4, \tag{26}$$

where E denotes the excess energy and f_1 is an (almost) universal function of E/Z^2. For the double-to-single ratio a similar relation holds,

$$R_Z(E) = f_2(E/Z^2)/Z^2. \tag{27}$$

To demonstrate the quality of our model with respect to the isoelectronic sequence, we show the scaled double-to-single ratios Z^2R_Z for Li^+, Be^{++}, C^{4+}, and O^{6+} compared to the *R*-matrix calculations of van der Hart and Feng [4] and Meyer *et al.* [5] in Fig. 5. For the lithium ion, we have also plotted the data of Kheifets and Bray (KB) [20] obtained with the convergent close coupling (CCC) method. A close inspection reveals that the *R*-matrix data appears to be systematically lower for all the ratios shown whereas the KB data, available for Li^+ only, differs from our results by 5% at most.

VI. DIFFERENTIAL QUANTITIES AND THE LACK OF INTERFERENCE TERMS

A. Singly differential cross sections

So far we have only considered integral quantities. For this purpose, it has been sufficient to formulate projectors onto the double-ionization space without referring to the atomic dipole, which couples the atom to the electric field of the photon. The photon coupling to the atom has been taken care of by using the total photoabsorption cross section in Eqs. (1) and (23). This remains true for singly differential cross sections (SDCS) with respect to the individual energy of the electrons, $d\sigma^{++}/d\varepsilon$, where ε is the energy of one of the electrons. As a generalization of Eq. (23), we may write the SDCS as

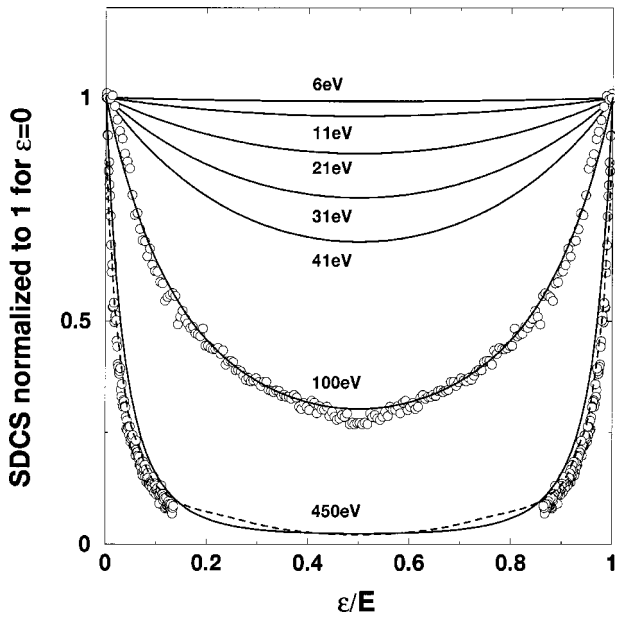

FIG. 6. Singly differential cross sections for various excess energies normalized to 1 for $\varepsilon=0$. Full lines: our results. Dashed line: calculations of Kheifets and Bray [18] at $E=450$ eV. Full circles: experimental data of Dörner and co-workers at $E=100$ eV and $E=450$ eV [18,49].

$$\frac{d\sigma^{++}}{d\varepsilon}=\sigma_{\mathrm{abs}}\left(\frac{dP_{\mathrm{KO}}^{++}}{d\varepsilon}+\frac{dP_{\mathrm{SO}}^{++}}{d\varepsilon}\right). \tag{28}$$

In Sec. II, we described the calculation of the classical double escape probability P_{KO}^{++}. To get the differential probability $dP_{\mathrm{KO}}^{++}/d\varepsilon$, we only have to additionally record the asymptotic energy ε of one of the emitted electrons. For this purpose, we divide the interval for ε which corresponds to double escape ($0\leqslant\varepsilon\leqslant E$) into N bins of equal size (we take $N=21$) and work out the differential probability by finding the trajectories that fall into the bins. For the SO mechanism the probability per unit energy P_{ε} [see Eqs. (14) and (18)], already gives $dP_{\mathrm{SO}}^{++}/d\varepsilon$.

Since the electrons are indistinguishable, the differential probabilities $dP_{X}^{++}/d\varepsilon$ must be symmetric about the equal-energy sharing point ($\varepsilon=E-\varepsilon=E/2$). In our treatment of both KO and SO, the two electrons are distinguishable (we talk of the primary and the secondary electron). Hence, the differential probabilities have to be symmetrized according to

$$\left.\frac{dP_{X}^{++}}{d\varepsilon}\right|_{\mathrm{sym}}=\frac{1}{2}\left(\frac{dP_{X}^{++}(\varepsilon,E)}{d\varepsilon}+\frac{dP_{X}^{++}(E-\varepsilon,E)}{d\varepsilon}\right). \tag{29}$$

In Fig. 6, we show the SDCS for a broad range of excess energies E. As can be clearly seen the SDCS is ''U shaped'' for all energies presented here in very good agreement with the calculations by Colgan *et al.* [19] (shown in Ref. [22]) and Kheifets and Bray [18] published only recently (see Fig. 6) and in poorer agreement with the older calculations [2]. Furthermore, our data agrees very well with the measurements of Wehlitz *et al.* (shown in Ref. [22]) and also with the recent data of Dörner and co-workers [18,49] (shown in Fig. 6). The experimental SDCS at 450 eV seems to be slightly steeper than ours. This is consistent with the slightly larger double-to-single photoionization ratio of Fig. 4 compared to experiment in this photon energy range. The discrepancy is likely due to neglected interference terms since exactly in this energy range SO and KO contributions are comparable (see inset of Fig. 4).

B. The role of interferences

For the way we have approached double-photoionization in terms of the quasiclassical knockout probability and the shakeoff as an additive quantum correction, interference does not play a role. However, coming from the most fundamental quantum-mechanical formulation, interference must be there if one separates a dynamical process into two contributions with identical final states. The corresponding amplitudes must be added coherently and upon taking the modulus square for probabilities interferences occur.

Since our results are in good agreement with experiment, although we have ignored interferences, they must play only a minor role. Support for this hypothesis comes from angular resolved experiments [50] as well as corresponding calculations [19,21,23,50,51]. SO and KO appear to be almost ''orthogonal'' with respect to their angular characteristics, i.e., the SO amplitude is large for detection of electrons at angles where the KO amplitude is small and vice versa. More formally expressed, let $A_{\mathrm{KO}}(\omega,\varepsilon,\Omega_1,\Omega_2)$ be the scattering amplitude to find, after absorption of a photon with frequency ω, one electron with energy ε at an angle Ω_1 and the other at an angle Ω_2, and let $A_{\mathrm{SO}}(\omega,\varepsilon,\Omega_1,\Omega_2)$ be the corresponding amplitude for shakeoff. Then, the fully differential cross section is given by

$$\frac{d\sigma}{d\varepsilon d\Omega_1 d\Omega_2}=|A_{\mathrm{KO}}+A_{\mathrm{SO}}|^2. \tag{30}$$

Forming singly differential cross sections from Eq. (30) by integration over the angles leads to

$$\frac{d\sigma}{d\varepsilon}=\frac{d\sigma^{++}}{d\varepsilon}+\sigma'(\varepsilon), \tag{31}$$

where $d\sigma^{++}/d\varepsilon$ is given by Eq. (28). Since both amplitudes peak in very different regions of (Ω_1,Ω_2) the interference term

$$\sigma'(\varepsilon)=\int A_{\mathrm{KO}}^{*}A_{\mathrm{SO}}d\Omega_1 d\Omega_2+cc \tag{32}$$

should be very small. This would explain the small effect of interferences in more integral cross sections, and would also validate from a different perspective the separation into the two processes, shakeoff and knockout. A closer look into an angular resolved formulation of knockout and shakeoff will be necessary to confirm this hypothesis.

VII. CONCLUSIONS

We have formulated a theoretical approach to double-photoionization of two-electron atoms in terms of two separate contributions, knockout and shakeoff. We could separate KO from SO since the former, modeled quasiclassically, does not contain SO parts. We could show that the KO probability is the part of the double-photoionization process which compares favorably with the electron-impact ionization cross section of the respective ion. This finding strengthens the half-collision model where, in general, a close relation between double-photoionization and electron-impact ionization of the ion had been proposed.

Viewed as a quasiclassical theory, shakeoff is a perturbation becoming dominant for large photon energies. It must be added to the quasiclassical double-photoionization cross section. Viewed from a quantum perspective, SO and KO should be added coherently on an amplitude level and interferences occur. The fact that they must be small (otherwise there would not be such a good agreement of our results with experiment and full numerical calculations) suggest that SO and KO indeed contribute for very different final-state variables dominantly. This renders the two processes almost distinguishable and justifies the separation of double-photoionization into these two mechanisms. This picture and interpretation of interferences can only be validated with angular resolved calculations that are planned for the future.

ACKNOWLEDGMENTS

We thank P. L. Chocian for his contribution in the early stages of this work, Andreas Becker and Thomas Pattard for valuable discussions, and the latter also for a critical reading of the manuscript. We are grateful to R. Dörner and his group for providing us with their results.

APPENDIX: CALCULATION OF THE WIGNER FUNCTION

We have implemented a simple and efficient method for calculating the Wigner function of the orbital $\psi(\boldsymbol{r}_2)$ [Eq. (6)] for the secondary electron. It was used by Dahl and Springborg [52] before and is based on the decomposition of $\psi(r_2)$ in terms of Gaussians,

$$\chi_\alpha(r_2)=(2\alpha Z_{\rm eff}^2/\pi)^{3/4}\exp(-Z_{\rm eff}^2\alpha r_2^2). \tag{A1}$$

The Wigner function of a wave function $\phi(\boldsymbol{r})$ is defined by [53]

$$\mathcal{W}_\phi(\boldsymbol{r},\boldsymbol{p})=\frac{1}{\pi^3}\int d^3\eta[\phi^*(\boldsymbol{r}_2-\boldsymbol{\eta})\phi(\boldsymbol{r}_2+\boldsymbol{\eta})\exp(2i\boldsymbol{p}\cdot\boldsymbol{\eta})]. \tag{A2}$$

In some special cases the integral in Eq. (A2) can be calculated analytically. One such example is the Wigner transformation of any sum of Gaussians, $\xi(r)=\Sigma_i c_i\chi_{\alpha_i}(r)$. One easily finds

TABLE II. Gaussian expansion coefficients and exponents used in the calculation of the Wigner function in Eq. (A3).

i	α_i	c_i
1	0.062157	0.107330
2	0.138046	0.339658
3	0.304802	0.352349
4	0.710716	0.213239
5	1.794924	0.090342
6	4.915078	0.030540
7	15.018344	0.008863
8	54.698039	0.002094
9	254.017712	0.000372
10	1776.775559	0.000044

$$\begin{aligned}\mathcal{W}_\xi(\boldsymbol{r},\boldsymbol{p})=&\frac{1}{\pi^3}\sum_{i=1}^{M}c_i^2\exp(-2Z_{\rm eff}^2\alpha_i r^2)\exp[-p^2/(2Z_{\rm eff}^2\alpha_i)]\\&+\frac{2}{\pi^3}\sum_{i>j}^{M}c_ic_j\left(\frac{\gamma_{ij}}{\alpha_i+\alpha_j}\right)^{3/4}\exp(-Z_{\rm eff}^2\gamma_{ij}r^2)\\&\times\exp[-p^2/(Z_{\rm eff}^2\alpha_i+Z_{\rm eff}^2\alpha_j)]\cos(2\tau_{ij}\boldsymbol{p}\cdot\boldsymbol{r}),\end{aligned} \tag{A3}$$

where M denotes the number of Gaussians, and the c_i's and α_i's are some constant coefficients and exponents. The γ_i's and τ_{ij}'s are given by

$$\gamma_{ij}=\frac{4\alpha_i\alpha_j}{\alpha_i+\alpha_j} \tag{A4}$$

and

$$\tau_{ij}=\frac{\alpha_i-\alpha_j}{\alpha_i+\alpha_j}, \tag{A5}$$

respectively. This nice property opens up an efficient way for calculating the Wigner function $\mathcal{W}_\psi$ of $\psi(r_2)$. From molecular-orbital calculations, Gaussian expansions of orbitals like $\psi(r_2)$ are well known. We find an $M=10$ Gaussian representation for $\psi(r_2)$ [54] to be sufficiently accurate for our purposes,

$$\psi(r_2)=\sum_{i=1}^{10}c_i\chi_{\alpha_i}(r_2). \tag{A6}$$

The Wigner function of $\psi(r_2)$ is then given according to Eq. (A3) with the appropriate coefficients and exponents listed in Table II.

[1] T.A. Carlson, Phys. Rev. **156**, 142 (1967); F.W. Byron and C.J. Joachain, *ibid.* **164**, 1 (1967).
[2] D. Proulx and R. Shakeshaft, Phys. Rev. A **48**, R875 (1993).
[3] M. Pont and R. Shakeshaft, Phys. Rev. A **51**, 494 (1995); J.-Z. Tang and I. Shimamura, *ibid.* **52**, R3413 (1995); Y. Qiu, J.-Z. Tang, J. Burgdörfer, and J. Wang, *ibid.* **57**, R1489 (1998).
[4] H.W. van der Hart and L. Feng, J. Phys. B **34**, L601 (2001).
[5] K. Meyer and C. Greene, Phys. Rev. A **50**, R3573 (1994); K. Meyer, C. Greene, and B. Esry, Phys. Rev. Lett. **78**, 4902 (1997); K. Meyer, Ph.D. thesis, University of Colorado, 1997 (unpublished).
[6] T. Åberg, Ann. Acad. Sci. Fenn., Ser. A4 **308**, 1 (1969); T. Åberg, Phys. Rev. A **2**, 1726 (1970).
[7] A. Dalgarno and A.L. Stewart, Proc. Phys. Soc. London **76**, 49 (1960); A. Dalgarno and H. Sadeghpour, Phys. Rev. A **46**, R3591 (1992).
[8] R.C. Forrey, H.R. Sadeghpour, J.D. Baker, J.D. Morgan, and A. Dalgarno, Phys. Rev. A **51**, 2112 (1995).
[9] R. Krivec, M.Y. Amusia, and V.B. Mandelzweig, Phys. Rev. A **62**, 064701 (2000).
[10] J.A.R. Samson, Phys. Rev. Lett. **65**, 2861 (1990); J.A.R. Samson, R.J. Bartlett, and Z.X. He, Phys. Rev. A **46**, 7277 (1992).
[11] J. McGuire, N. Berrah, R. Bartlett, J. Samson, J. Tanis, C.L. Cocke, and A.S. Schlachter, J. Phys. B **28**, 913 (1995).
[12] J.S. Briggs and V. Schmidt, J. Phys. B **33**, R1 (2000), and references therein.
[13] J.C. Levin, D.W. Lindle, N. Keller, R.D. Miller, Y. Azuma, N.B. Mansour, H.G. Berry, and I.A. Sellin, Phys. Rev. Lett. **67**, 968 (1991); J.C. Levin, G.B. Armen, and I.A. Sellin, *ibid.* **19**, 1220 (1996).
[14] R. Wehlitz, F. Heiser, O. Hemmers, B. Langer, A. Menzel, and U. Becker, Phys. Rev. Lett. **67**, 3764 (1991).
[15] J.A.R. Samson, W.C. Stolte, Z.-X. He, J.N. Cutler, and Y. Lu, Phys. Rev. A **57**, 1906 (1998).
[16] R. Dörner *et al.*, Phys. Rev. A **57**, 1074 (1998).
[17] R. Dörner, V. Mergel, O. Jagutzki, L. Spielberger, J. Ullrich, R. Moshammer, and H. Schmidt-Böcking, Phys. Rep. **330**, 95 (2000), and references therein.
[18] A. Knapp *et al.*, Phys. Rev. Lett. **89**, 033004 (2002).
[19] J. Colgan, M.S. Pindzola, and F. Robicheaux, J. Phys. B **34**, L457 (2001); J. Colgan and M.S. Pindzola, Phys. Rev. A **65**, 032729 (2002).
[20] A.S. Kheifets and I. Bray, Phys. Rev. A **54**, R995 (1996); **57**, 2590 (1998); **58**, 4501 (1998); J. Phys. B **31**, L447 (1998).
[21] L. Malegat, P. Selles, and A.K. Kazansky, Phys. Rev. A **60**, 3667 (1999); Phys. Rev. Lett. **85**, 4450 (2000); P. Selles, L. Malegat, and A.K. Kazansky, Phys. Rev. A **65**, 032711 (2002).
[22] T. Schneider, P.L. Chocian, and J.-M. Rost, Phys. Rev. Lett. **89**, 073002 (2002).
[23] A.Y. Istomin, N.L. Manakov, and A.F. Starace, J. Phys. B **35**, L543 (2002).
[24] T. Pattard and J. Burgdörfer, Phys. Rev. A **64**, 042720 (2001).
[25] S. Keller, J. Phys. B **33**, L513 (2000).
[26] A.S. Kheifets, J. Phys. B **34**, L247 (2001).
[27] J.A. Tanis *et al.*, Phys. Rev. Lett. **83**, 1131 (1999).
[28] F. Bloch, Phys. Rev. **48**, 187 (1935).
[29] M.Y. Amusia and A.I. Mikhailov, J. Phys. B **28**, 1723 (1995).
[30] T.Y. Shi and C.D. Lin, Phys. Rev. Lett. **89**, 163202 (2002).
[31] T.D. Thomas, Phys. Rev. Lett. **52**, 417 (1984).
[32] J.A.R. Samson, Z.X. He, L. Yin, and G.N. Haddad, J. Phys. B **27**, 887 (1994).
[33] J.-M. Rost, J. Phys. B **28**, L601 (1995).
[34] R. Abrines and I.C. Percival, Proc. Phys. Soc. London **88**, 861 (1966).
[35] E.J. Heller, J. Chem. Phys. **65**, 1289 (1976).
[36] D.J.W. Hardie and R.E. Olson, J. Phys. B **16**, 1983 (1983); D. Eichenauer, N. Grün, and W. Scheid, *ibid.* **14**, 3929 (1981); J.S. Cohen, *ibid.* **18**, 1759 (1985); C.O. Reinhold and C.A. Falcón, Phys. Rev. A **33**, 3859 (1986).
[37] T. Geyer and J.-M. Rost, J. Phys. B **34**, L47 (2001); **35**, 1479 (2002).
[38] D.A. Waason and S.E. Koonin, Phys. Rev. A **39**, 5676 (1989).
[39] C.H. Keitel and P.L. Knight, Phys. Rev. A **51**, 1420 (1995); D. Bauer, *ibid.* **56**, 3028 (1997); G. van de Sand and J.-M. Rost, Phys. Rev. Lett. **83**, 524 (1999).
[40] L.-B. Fu, J. Liu, J. Cheng, and S.-G. Chen, Phys. Rev. A **63**, 043416 (2001); V.R. Bhardwaj, S.A. Aseyev, M. Mehendale, G.L. Yudin, D.M. Villeneuve, D.M. Rayner, M.Y. Ivanov, and P.B. Corkum, Phys. Rev. Lett. **86**, 3522 (2001).
[41] N. Henriksen, Adv. Chem. Phys. **91**, 433 (1995); J.-M. Rost, Phys. Rep. **297**, 271 (1998).
[42] P.K. Kabir and E.E. Salpeter, Phys. Rev. **108**, 1256 (1957).
[43] P. Kustaanheimo and E. Stiefel, J. Reine Angew. Math. **218**, 204 (1965); S.J. Aarseth and K. Zare, Celest. Mech. **10**, 185 (1974).
[44] A.B. Peart, D.S. Walton, and K.T. Dolder, J. Phys. B **2**, 1347 (1969).
[45] T. Kato, Commun. Pure Appl. Math. **10**, 151 (1957).
[46] T. Surić, K. Pisk, and R.H. Pratt, Phys. Lett. A **211**, 289 (1996).
[47] A.L. Stewart and T.G. Webb, Proc. Phys. Soc. London **82**, 532 (1963).
[48] M.A. Kornberg and J.E. Miraglia, Phys. Rev. A **49**, 5120 (1994).
[49] A. Knapp *et al.*, J. Phys. B **35**, L521 (2002).
[50] H. Bräuning *et al.*, J. Phys. B **31**, 5149 (1998).
[51] M. Pont, R. Shakeshaft, F. Maulbetsch, and J.S. Briggs, Phys. Rev. A **53**, 3671 (1996).
[52] J.P. Dahl and M. Springborg, Mol. Phys. **47**, 1001 (1982).
[53] E.P. Wigner, Phys. Rev. **40**, 749 (1932).
[54] F.B. van Duijneveldt, IBM Research Report No. RJ945, 1971, p. 46.